19th Australasian Fluid Mechanics Conference
Melbourne, Australia
8-11 December 2014

Heat Transfer Prediction of a Turbine Stage using Fluid-Thermal-Structural Interaction Simulation

I.A. Ubulom[1], A.J. Neely[1] and K. Shankar[1]

[1] School of Engineering and Information Technology
University of New South Wales, Canberra, ACT 2600, Australia

Abstract

The market competitiveness of gas turbine engines has resulted in a drastic drive for improved efficiency, performance, and structural durability. With the economically expensive nature of experimental rig data measurements, numerical modelling tools prove indispensable especially during the early component design stage. While there are growing interests in numerical prediction of thermal loads on the turbine stage, the classical approach of neglecting the interactions between the aerodynamic, thermal and structural domains may not accurately represent the problem. For this work, the initial steps in a coupled simulation approach involving aerodynamic, thermal and structural fields to estimate the temperature and heat loads in the turbine stage are established. The correct representation of the physics in this domain offers improved fidelity in heat transfer and temperature prediction of the turbine blade which can lead to an improvement in component life prediction. The commercial FEM solver ANSYS is used for the thermal heat conduction problem while a finite volume solver, CFX is used for the aerodynamic load prediction. The predictions are compared against an experimental test case.

Introduction

With the ongoing advancement in computing resources, numerical modelling has become an indispensable tool in temperature and heat transfer prediction of gas turbine blades. In a typical high pressure turbine stage, there is a complex interplay between the severe rotational stress resulting from high speed component rotation, the strong aerodynamic loads and the high combustor exit temperatures, to which the turbine blade material is subjected to. Numerical simulations of the thermal interactions between the fluid flow and the blade structure offer new design paths to reduce cost related to design through the reduction of the number of experimental tests needed, [4]. Recently, [22] noted the need for adoption of a multidisciplinary approach in numerical predictions where the aerodynamic analysis needs coupling to the thermal and structural stress fields. Such propositions are buttressed by the few experimental test cases of turbine heat transfer and temperature predictions available in the public domain, [19], [6].

For turbine blade heat transfer, a coupled field analysis of conjugate heat transfer (CHT) has been recently been widely adopted. [11] used a CHT approach for prediction of film cooling effectiveness on a gas turbine vane. [13] adopted the monolithic approach for turbine blade cooling analysis. [1] presented a 3D CHT analysis for heat transfer predictions on turbine blade investigating the effect of geometry de-featuring in the end-wall region of a turbine blade. For the result presented, on the blade pressure side, the slowing of the gas caused a thickening of the boundary layer which resulted in reduction in heat transfer. The highest heat transfer was noted at the stagnation location of the leading edge where the boundary layer tails off, reducing the thermal resistance at that location. [17] applied a finite volume fluid solver for conjugate heat transfer of a film cooling device with solid conduction specified through a user subroutine code that defines the Fourier heat conduction equation in the fluid solver. Other areas of increasing use of coupled field simulation on blade flow and heat transfer are reported in [12], [14],[17] etc. While the accurate resolution of boundary layer is important, the application of LES method for the fluid flow analysis and its incorporation in readily available CHT solver is however considered a milestone away, [20]. For this study, the closure to fluid equation is through the SST k-ω model implemented in CFX.

While the CHT method is continuously being improved for heat transfer prediction, the incorporation of additional solution to the structural mechanics equation by incorporating the solid domain discretization in the fluid solver and vice versa is yet to be fully implemented. Such is necessary as to accounts for the possible interactions between the fluid and solid domains. In the solid domain, mesh deformation and structural displacement is solved and transferred to the fluid domain where wall heat flow and velocity flow is transferred back to the solid domain. This being the basis of a coupled fluid-thermal structural analysis ensures the conservation of fluxes at the fluid-solid interface. This work therefore adopts a fluid-thermal-structural interaction approach to solve a heat transfer problem for a turbine stage. In addition to accounting for the likely interactions between the various domains, the effects of upstream stator on the flow field and heat transfer boundary treatment of the turbine stage are analysed. Further insight is also provided on the underlying mechanism and influence of secondary flow phenomena on the turbine blade heat transfer problem.

Experimental Test Case

The test case considered is the Aachen turbine configuration consisting of 3-subsonic blade rows with 36-41-36 blade counts making up the 1.5 stages. As reported by [24], the configuration was tested for mass flow rates of 7 kg/s and 8kg/s. For this study, the 1st-stage was considered. Table.1 illustrates the boundary conditions and geometric parameters as presented by [7]

The test condition simulated is representative of a low pressure turbine (LPT) stage. Such blade characteristics may experience laminar-turbulent transition due to possible separation, [10]. In that case, the largest adverse pressure gradient is imposed immediately after transition at such point where the turbulent boundary layer is thinnest with least possibility of flow separation. The predictions in this study work are therefore compared against experimental measurements of [8].

Parameters	Stator	Rotor
Pitch @ Midspan	47.6mm	41.8mm
Blade Number	36	41
Reynolds number	6.8 x 10^5	4.9 x 10^5
Rotational Speed	-----	3500rpm
Tip Diameter	600mm	600mm
Inlet Blade Angle	0^0	40.7^0
Inlet Total Pressure	155kPa	-----
Inlet Temperature	308K	-----
Exit Mach number	0.45	----

Table 1. Turbine stage parameters

Numerical Approach

The finite volume code ANSYS CFX was used for fluid flow solutions. The inviscid fluxes are approximated through the Roe's scheme while the viscous fluxes are approximated through the central differencing scheme. To accelerate convergence of the solution to steady state, a local time stepping is employed while the time accurate solution of the unsteady flow is obtained in the second order accurate dual time stepping approach. Turbogrid was used to generate the grid for the fluid domain using an overlapping O-H grid on both the stator and rotor geometry. The O-grids were clustered around the airfoil surfaces to resolve the boundary layers while adequate H-grid lines were mapped for proper resolution of the wake in the interblade row areas. For the solid domain, the geometry was discretised with tetrahedral SOLID227 elements. To accurately model the required thermal degree of freedom, a user subroutine code was implemented to modify the element degrees of freedom suitable for the coupled physics simulation. The SST k-ω model was used to provide closure for the turbulent stress and heat flux. An automatic wall treatment was used which allows the high gradient shear layers near the wall to be modelled without restrictions to fine mesh in the region. This enables a substantial saving in CPU time and storage and ensures a gradual switch between wall functions and low Reynolds number grid without loss of accuracy maintaining a wall grid resolution of $y^+ < 2$ in the boundary layer. To interpolate the fluxes and loads between the domains, a fluid-solid interface was specified on the suction and pressure surfaces of both the stator and rotor.

In the solid domain, a fixed surface boundary condition was maintained at the root region of the geometries while the rotational velocity of 367 rad/s was specified on the Z-axis of the rotor. An Initial wall temperature of 280-K was specified on the stator and rotor thus maintaining temperature ratio of 0.7 with the convective gas temperature. The solution was solved while monitoring the RMS residuals to 10^{-5}.

To estimate heat conduction in the solid domain, CFX uses the conservation of energy equation to account for heat transport.

$$\frac{\vartheta(\rho h)}{\vartheta t} + \nabla.(\rho U_s h) = \nabla.(\lambda \nabla T) + S_e \qquad (1)$$

In equation (1), the terms h, ρ and λ represent the enthalpy, density and the material' thermal conductivity. U_s represents the motion of the solid element (rotor) with respect to the reference frame. At the fluid-solid interface, the solver uses a hybrid interpolation to calculate the surface temperature based on the flux conservation equation for the control surface. This is done in a manner that eliminates any discontinuity in the temperature values. The term S_e is the volumetric heat generation term. In this case, $S_e = 0$ Noting the differences in the time-scales between the fluid and solid, the solution time-step was limited by the fluid solver while convergence of fluxes were monitored through stagger iterations between the fluid and solid domains. The solution convergence was monitored when the flux and temperature variations were below 0.01.

For the solution in the finite element solver, with rotational velocity applied to the rotor domain, the equation of motion for an elastic structure is modified as shown in equation (2) in a manner earlier proposed by [4] as;

$$[M]\{\ddot{q}\} + ([C] - \Omega[C^c]\{\dot{q}\} + ([K] - \Omega^2[K^c])[q] = \{f\} + \Omega^2[K^c]\{q_0\} \qquad (2)$$

Where Ω is the natural frequency of the blade. The term $\{q_0\}$ in equation (2) is the position vector of the particle in stationary system while {q} is the displacement. The terms representing the rotational velocity effects are $\Omega[C^c]\{\dot{q}\}$, $\Omega^2[K^c]\{q_0\} + \{q\}$ due to Coriolis and centrifugal forces. With the highly three-dimensional nature of turbine blades, such "aerothermo-elasticity" problems are highly nonlinear, thus requiring geometric nonlinear theory of elasticity, [20].

Results

Figure 1 shows the predicted pressure coefficient distributions for the stator and rotor geometries compared with experimental measurements. Also shown are earlier predictions by [8] obtained using non-viscous stream surface calculation. Pressure gradients near the leading edge of the turbine airfoil are generally attributed to stagnation and surface curvature effects, [15]. For the case here of a full stage, interblade row effects also contribute to the displacement of the stagnation point onto the pressure side of the rotor blade. After an initial leading edge spike, the pressure remains relatively constant between 20-50% of the stator pressure surface. On the suction surface, a steep descent with strong favourable pressure is maintained up to the 70% position while a slight adverse pressure slope follows to the trailing edge of the stator blade suction side. Flow separation is only observed at the very trailing for both the stator and rotor blades

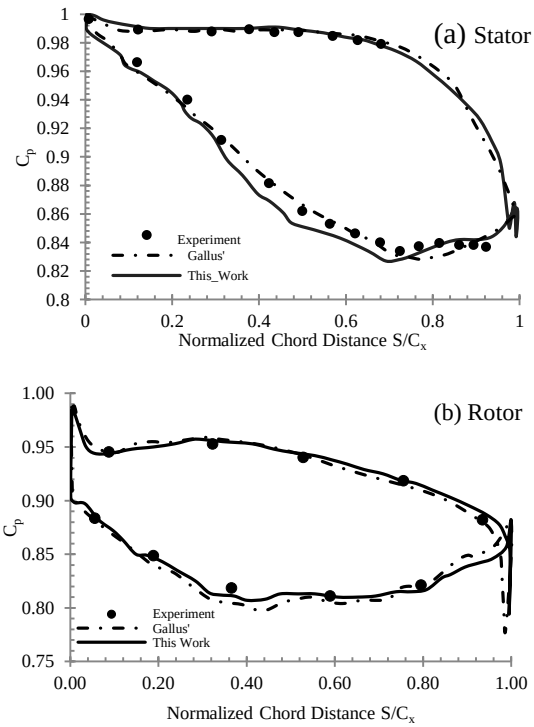

Figure 1. Coefficient of pressure distributions (a) Stator (b) Rotor blades

By observing the ratio of the length of favourable pressure gradient to adverse pressure gradient, the stator airfoil is shown to be loaded in the forward position. For the rotor, it is highly loaded in the aft portion on the pressure side. On the suction surface of the rotor blade, the favourable pressure gradient is maintained to about 30-chord position while the adverse pressure is seen from the position at 80% to the trailing edge. The overall predictions show a close match with experimental data with little variation on the suction side of the stator blade. This variations in this region are mainlye attributed to additional radial pressure gradient developed in an annular cascade as compared to the measurements in linear cascade, [2].

At the trailing edge of the rotor blade there is unsteadines in the flow leading to vortex shedding. Due to the fine mesh used at the trailing edge, the flow tries to approach a stagnation point on the trailing edge radius, thus the Kutta condition is not well met. The flow accelerates on both surfaces at the trailing edge thus leading to a negative loading at this region. These conditions are likely even with steady Navier-Stokes solvers which should allow the flow to separate before accelerating but in practice are rarely experienced, [3]. Such trailing edge behaviour is therefore never found in experimental observations.

Heat transfer Results

Figure 2 illustrates the convective heat transfer coefficient plot of the fluid-interface for the stator and rotor respectively showing both the suction side (-1 to 0) and the pressure surface (0 to 1) with 0 being the leading edge. The Prandtl number describing the relative thickness of the velocity and thermal boundary layers was fixed by assuming a constant value of 0.7. The flow is modelled with Inlet Turbulence intensity of 5%, being a moderately assumed value for turbine flows, [21]. The plots show in general the variation in heat transfer coefficient (htc) which is nominally related to the pressure coefficient distribution around the blade. The htc is primarily driven by the convective transport of fluid motion in the stream direction and fluid conduction properties at close to the wall, in the boundary layer.

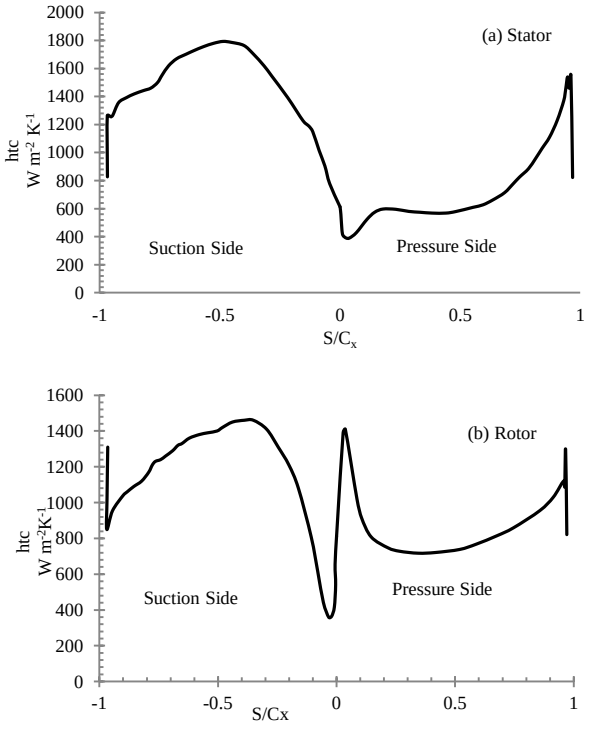

Figure 2. Heat transfer coefficient predictions for (a) Stator (b) rotor

For the stator, the pressure distribution in figure 1 showed a rapid acceleration after the initial stagnation location on the suction surface up to about 60-70% chord position. Such conditions are conducive to maintaining a fully attached flow on the surface with the point of lowest pressure on the suction surface almost coinciding with the peak velocity. The resulting heat transfer coefficient becomes a function of this velocity distribution distribution and the developing thermal boundary layer. After the peak acceleration, the adverse pressure gradient drives the lower momentum fluid over the surface thereby thickening the boundary layer which leads to a stready decrease in heat transfer coefficient. While the flow is modeled as fully turbulent, the strong facvourable pressure gradient on the suction surface tends to relaminarize the flow. Such effects are also reported by [23]

On the rotor surface in figure 2b, the heat transfer coefficient is strongly driven by leading edge radius, interblade row effects and freestream turbulent intensity. At the rotor leading edge, the ensemble-avearged htc is enhanced by the increase in turbulence intensity due to the passing wakes from the upstream stator. After the initial increase at the leading edge, on the pressure surface of the rotor blade, the heat transfer coefficient decreases slightly between 20-40% chord length. A steady rise also commences from about the 45% position. As noted earlier, the non-uniform stator exit flow coupled with the varying circumferential speed across the blade spanwise direction leads to a displacement of the stagnation point. In fact, in the experiment by [8], it was reported that while the rotor blade experiences a low circumferential speed, there is an increasing stator outlet velocity which moves the stagnation to the pressure side with a resulting flow acceleration noticed at the leading edge towards the suction side region. This is also apparent in figure 2 where the acceleration causes a steady rise in heat transfer coefficient following the LE portion of the suction surface.

Figure 3 shows the strong influence of secondary flow features on the blade wall heat transfer prediction. “A” indicates the leading edge horseshoe vortices (Suction side leg) that merge downstream of the blade surface with the pressure side leg vortices from adjacent blades to form the passage vortex. “B” indicates the tip clearance vortex due to the pressure gradient existing between the pressure and suction surface of the blade respectively. The horseshoe vortex occurs as a result of spanwise pressure gradient in the vicinity of the blade’s leading edge, for both the stator and rotor.

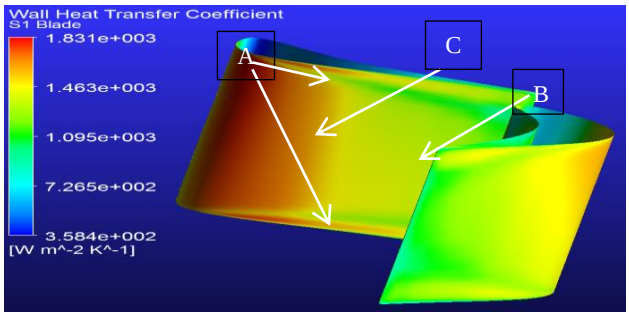

Figure 3. Influence of secondary flow patterns on blade heat transfer coefficient prediction looking upstream from the rotor

The strong vortical motion of the pressure side leg of the horseshoe entrains most of the fluid in the incoming boundary. The fluid therefore moves toward the suction surface where it merges with the suction side counterpart and lifts off the blade surface thereby causing a reduced thermal resistance with the formed thin boundary layer

This leads to a high blade wall heat transfer coefficient in this region as it convects towards the midspan region at the passage exit. The movement of this vortex towards the midspan location

is influenced by the unsteady nature of flow. Thus the stator exit secondary flow field interacts with that of the rotor field. For the tip clearance vortex B, it is forced towards the blade wall region on the suction surface where the counter rotating nature of its stream line tails off the lower momentum flow on the blade wall thus leading to a high heat transfer coefficient in this region. The region indicated by C however is attributed to a reduced wall shear stress following high suction in the high speed region on the suction surface. A Similar feature was reported by [9]. Overall, the heat transfer coefficient around the blade is highly influenced by the wall pressure distribution and secondary flow effects. Further detailed analysis using boundary layer parameters such as shape factor (ratio of the displacement thickness to momentum thickness) can be used to estimate the intermittency characteristics in the boundary layer.

Conclusions

Coupled fluid-thermal-structural interaction was adopted to predict heat transfer loads on a turbine stage, assuming an isothermal wall as an initial step. Although the additional equation of solid motion is solved in this coupled analysis the displacement in this case was negligible. The heat transfer to the blade was a strong function of convective fluid transport and secondary flow features around the blade. Further detailed analysis is required to estimate boundary layer properties in the blade wall region for a non-isothermal wall where the influence of coupled field simulation will likely alter the heat transfer distribution, and thus the eventual lifing of the blade.

Acknowledgement

This work was partially supported by Total E&P Nigeria Ltd.

References

[1] Andreini. A, Carcasci C, Facchini. B, Stecco S., Ciani .A, Innocenti L. and Bonini A, "*Conjugate heat transfer calculations on a GT rotor blade for industrial applications part II*: Improvement of external flow modeling," in *GE Technology Insights*, Copenhagen, Denmark, 2012.

[2] Acharya.S, Mahmood Gazi " Turbine Blade Aerodynamics" Publication of the Louisana State University, Department of Mechanical Engineering. USA

[3] Denton J, Dawes W, "Computational fluid dynamics for turbomachinery design," in *Proceedings of the Institution of Mechanical Engineers, Part C:* , 1998

[4] Doi H, "Fluid/Structure Coupled Aeroelastic Computations for Transonic Flows in Turbomachinery," A PhD Dissertation of Stanford University, USA, 2002

[5] Duchaine F, A. Corpron, L. Pons, V. Moureau, F. Nicod and T. Poinsot, "Development and Assessment of a coupled strategy of Conjugate heat transfer with Large Eddy Simulation," *International Journal of heat and Fluid flow Vol.30*, pp. 1129-1141, 2009.

[6] Dunn M, "Detailed Heat-Flux Measurements for the Blade Surface in a Full-Stage Rotating Turbine," *American Society of Mechanical Engineers*, pp. Paper 86-GT-77, 1986

[7] Gallus H, Weskamp K, Zeschky J, "Computational Predictions and Measurements of the Axial Flow Turbine Cascade and Stages," in *Secondary Flows in Turbomachines*, Luxembourg, AGARD Conference Proceedings No.469, 1990, p. Chapter 21

[8] Gallus H, Zeschky J. Hah C, "Endwall and Unsteady Flow Phenomena in an Axial Turbine Stage," *39th International Gas Turbine and Aeroengine Congress and Exhibition*, pp. 94-GT-143, 1994

[9] Hodson H, Coull J, Thomas R, "Velocity Distribution for Low Pressure Turbines," *Journal of Turbomachinery*, pp. 1-13,Paper ID GT2010-041006, 2010

[10] Hodson H, Dominy R, "Three-Dimenisonal flow in a Low Pressure Turbine Cascade," *Journal of Turbomachinery*, vol. 109, pp. 177-185, 1998

[11] Kassab. A., E. Divo, J. Heidman, E. Steinthorsson and F. Rodriquez, "BEM/FVM Conjugate heat transfer analysis for a film cooled turbine blade," *International Journal of Numerical Methods for Heat and Fluid Flow*, pp. Volume 13, No.5, Pages 581-610, 2003

[12] Kim K. M., Park J. S, Lee D. H., Lee T. W. and Cho H. H., "Ananlysis of Conjugate heat transfer, stress and failure in gas turbine blade with circular cooling passages," *Engineering Failure Analysis 18*, pp. 1212-1222, 2011

[13] Latorre S. S, "A Conjugate heat transfer method for turbine cooling," A PhD thesis od Politecnico Di Bari, SSD-IND/08, 2011

[14] Maheu N, Moureau V, Domingo P, Dunchaine F. and Balarac G, "Large Eddy Simulations of flow and heat transfer around a low-Mach number Turbine Blade," in *Center for Turbine Research, Proceedings of Summer Program*, 2012

[15] Mayle R. E, "The role of laminar-turbulent transition in gas turbine engines," *International Journal of Turbomachinery*, pp. 509-536, Volume 113, October 1991

[16] Mensch A, Thole K. A, Craven B. A, "Conjugate Heat transfer Measurements and Predictions of a Blade Endwall with a thermal Barrier Coating," in *Proceedings of the ASME Turbo Expo, Turbine Technical Conference*, Dusseldorf, 2014

[17] Montomoli F, Adami P, Martelli F, "A Finite Volume Merthod for Conjugate heatr transfer in film cooling Devices," *Publication of Department of Energy, Univeristy di Firenze*, Italia, 2012

[18] Pletcher R. H, Tannehil J. and Anderson D. A, Computational Fluid Mechanics and Heat Transfer, Boca Rato London New York: CRC Press, Taylor and Francis Group, 2013

[19] Rao.K, R. Delaney and M. G. Dunn, "Vane blade interaction in a transonic turbine. Part II: heat transfer," *Journal of Propulsion and Power*, pp. 312-317, 1994

[20] Reddy T, Bakhle M, Srivastava R. and Mehmed O, "APPLE: An Aeroelastic Analysis System for Turbomachines and Propfans," *American Institute of Aeronautics and Astronauts*, no. AIAA-92-4712-CP, pp. 207-225, 1992

[21] Schobeiri.M.T, Ozturk.B, Kegali M., Bensing D. "On the Physics of Heat transfer and Aerodynamic Behaviour of Seperated Flow Along a Highly Loaded Low Pressure Turbine Blade Under Periodic Unsteady Wake Flow and Varying of Turbulence Intensity" *Journal of Heat Transfer*, Vol.130, paper number: 051703, page 1-20

[22] Tucker.P, "Computations of Unsteady Turbomachinery Flows. Part 1: Progress and Challenges," *Aerospace Sciences*, pp. Volume 47: 522-545, 2011.

[23] Turner A, "Local heat Transfer Measurement on Gas Turbine Blades," *Journal of Mechanical Engineering*, vol. 13, pp. 1-13, 1971

[24] Yao J, Davis R, Alonso J, Jameson A., "Unsteady Flow Investigations in an axial turbine using the massively parallel flow solver," *39th AIAA Aerospace Sciences Meeting and Exhibit*, pp. 1-14, AIAA 2001-0529, 2001